Metalurgi (2019) 2: 91 - 98

LIPI

METALURGI

Available online at www.ejurnalmaterialmetalurgi.com

CARBURIZATION STUDY ON A FIRED HEATER TUBE OF A PETROLEUM PROCESSING REFINERY

Dewa Nyoman Adnyana

Department of Mechanical Engineering, Faculty of Industrial Technology
National Institute of Science and Technology (ISTN), Jakarta, Indonesia
*****E-mail : adnyanadn@yahoo.com

Masuk Tanggal : 31-10-2019, revisi tanggal : 05-11-2019, diterima untuk diterbitkan tanggal 05-11-2019

Intisari

Dapur pemanas pada sebuah kilang pengolahan minyak bumi mengalami kebocoran pada salah satu pipa konveksi. Pipa tersebut terbuat dari baja karbon rendah jenis ASTM A-106 Gr.B. Cairan proses di dalam pipa adalah xylene dengan tekanan desain 15,8 kg/cm²g dan suhu desain yaitu 299 °C (pada saluran masuk) dan 405 °C (pada saluran keluar). Penelitian ini bertujuan untuk menentukan jenis dan faktor penyebab serta mekanisme terjadi kebocoran pada pipa tersebut. Sejumlah pengujian telah dilakukan meliputi pemeriksaan visual dan makroskopik, analisa kimia, pengujian metalografi dan kekerasan, serta analisa SEM (*scanning electron microscopy*) yang dilengkapi dengan EDS (*energy dispersive spectroscopy*). Hasil penelitian yang diperoleh menunjukkan bahwa kebocoran yang terjadi pada pipa konveksi disebabkan oleh karburisasi dan pembentukan debu/serbuk logam. Karburisasi terjadi pada dinding bagian dalam pipa yang mengalami panas berlebih secara lokal akibat terbentuknya endapan kokas.

Kata Kunci: Pipa konveksi, karburisasi, endapan kokas, panas berlebih secara lokal, pembentukan debu logam

Abstract

The fired heater of a petroleum processing refinery leaks in one of the convection tubes. The tube is made of ASTM A-106 Gr.B. Process fluid in the tube is xylene with a design pressure of 15.8 kg/cm²g and design temperature of 299 °C (at the inlet) and 405 °C (at the outlet). This study aims to determine the type and causes and the mechanism of leakage in the tube. A number of tests have been carried out including visual inspection and macroscopic analysis, chemical analysis, metallographic and hardness testing, and SEM (scanning electron microscopy) analysis which is equipped with EDS (energy dispersive spectroscopy). The results obtained showed that the leak that occurred in the convection tube was caused by carburization and metal dusting. Carburization occurs in the inner walls of the tube that experience some localized overheating due to the formation of coke deposits.

Keywords*: Convection tube, carburization, coke deposits, localized overheating, metal dusting*

1. INTRODUCTION

Carbon steels with ferrite-pearlite microstructures are used extensively at elevated temperatures in petroleum-processing plants, chemical processing plants, fossil-fired power generating plants, etc. [1]-[2]. Besides, interest in carbon steels and other ferritic steels has increased because their relatively lower thermal expansion coefficient and higher thermal conductivity make them more attractive than austenitic steels in the application where thermal cycling is present [3].

Carbon steels are the predominant materials in the fabrication of fired heater, pressure vessel, etc., because of their low cost, versatile mechanical properties, and availability in fabricated forms. They are the most common materials used in a noncorrosive environment in the temperature range of -29 to 425 °C in oil refineries and chemical plants [1]. Although the ASME code gives allowable stresses for temperatures higher than 425 °C, it also notes that prolonged exposure at these temperatures may result in the carbide phase of the carbon steels being converted to graphite. This phenomenon, known as graphitization, is a cumulative process dependent on the time the material is at or above 425 °C [4]. The result is a weakening of the steel after higher-temperature exposure. Carbon steels are also increasingly affected by creep at temperatures above 370 °C, especially when the steels experience some carbide spheroidized [3]-[4].

In the carburizing environment at the elevated temperatures, the decomposition of carburizing gases or carbonaceous material can release the carbon atoms, which can allow diffusion of carbon into the steel to form a hard, brittle structure at the surface that may crack or spall upon cooling. This phenomenon, known as carburization, can result in the loss of high temperature creep ductility, loss of ambient temperature mechanical properties, loss of weld-ability, and corrosion resistance [5]-[9]. This carburization can be taking place either in some extensive area of the metal surface or only in some localized area or spot. In a more advanced stage, there may be a volumetric increase in the affected area, and some severe forms of carburization may occur. This is known as metal dusting, which considered to be a saturation of the metal matrix by carburization, precipitation of metal carbides at the metal surface and grain boundaries, and or decomposition of the metal carbides under the graphite and metal particles. Also, this metal dusting is characterized by rapid metal wastage and indicated by the formation of pits, which usually form on the surface and may contain soot or graphite dust [10]-[11]. This leads to the premature failure of equipment made from these steels, resulting in the unplanned shutdown in many industrial processes.

This paper presents a metallurgical assessment performed on a damaged convection tube of a fired heater of a petroleum processing refinery after it had been in service for more than 20 years. The tube was made of ASTM A-106 Gr. B, a standard specification for seamless carbon steel tube or pipe for high-temperature service. The tube diameter was 168.3 mm, while its wall thickness was 7.11 mm. The process fluid in the tube was xylene with the design pressure of 15.8 kg/cm2g and a design temperature of 299 °C (inlet) /405 °C (outlet). The failed tube was installed in a horizontal position in the heater and located at first row immediately above the radiant section. The failure comprised of two leakage holes that formed on its internal wall (see Fig.1). The type and factors that may have caused the leakage on the convection tube are discussed in this paper.

The purpose of this study was to determine whether the material used for the damaged convection tube met the specification or suitable for its operating condition. Furthermore, this study was also aimed to establish the type, cause, and mode of failure of the damaged convection tube, and based on the determination; some corrective or remedial action may be initiated that will prevent a similar failure in the future.

2. EXPERIMENTAL METHOD

In this study, several specimens were prepared from the as-received damaged convection tube for laboratory examination. A macroscopic examination on the damaged area was performed using a stereomicroscope. Chemical analysis of the prepared sample was carried out using an optical spark emission spectrometer. The purpose of this chemical analysis was to determine whether the material used for the damaged convection tube meets the specification. Besides, metallographic examinations were also performed on the prepared samples using an optical microscope at various magnifications. The scheme of specimen preparation for metallographic examination is given in Fig. 2, which included two areas of A and B. Area A is located approximately 180º or at the opposite side from the leakage hole of area B. The metallographic samples were cut away from the two areas in both transverse and longitudinal directions and mounted using epoxy and prepared by grinding, polishing, and etching. The etchant applied was 5% nital solution [11]. A hardness survey was also carried out on the same samples for the metallographic examination using the Vickers hardness method at a load of 5 kg (HV 5). Moreover, the examination of some surface deposits that formed either on the external or on the internal surfaces around the leakage hole area was also performed using SEM (scanning electron microscopy) to determine the deposit topography and nature of the failure. The SEM was also equipped with an EDS (energy dispersive spectroscopy) analysis to detect the presence of any corrosion by-product.

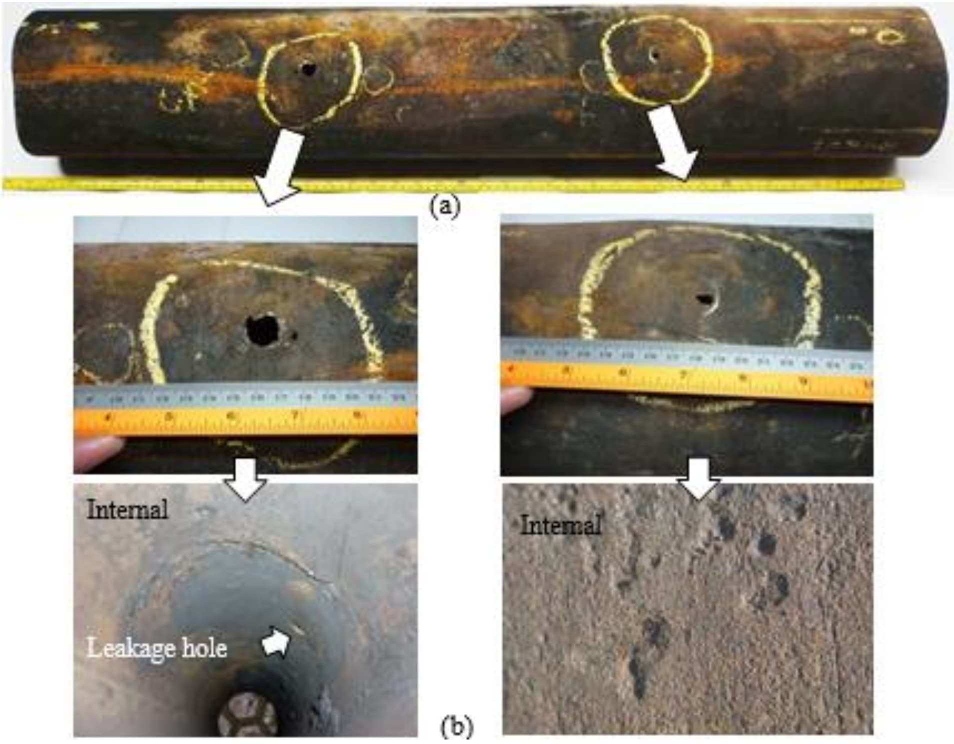

Figure 1. (a) As-received convection tube, showing two leakage holes that formed on the internal tube wall, (b) Close-up view of each of the two leakage holes shown in Fig.1(a), showing the damaged topology that formed around the tube inner surfaces

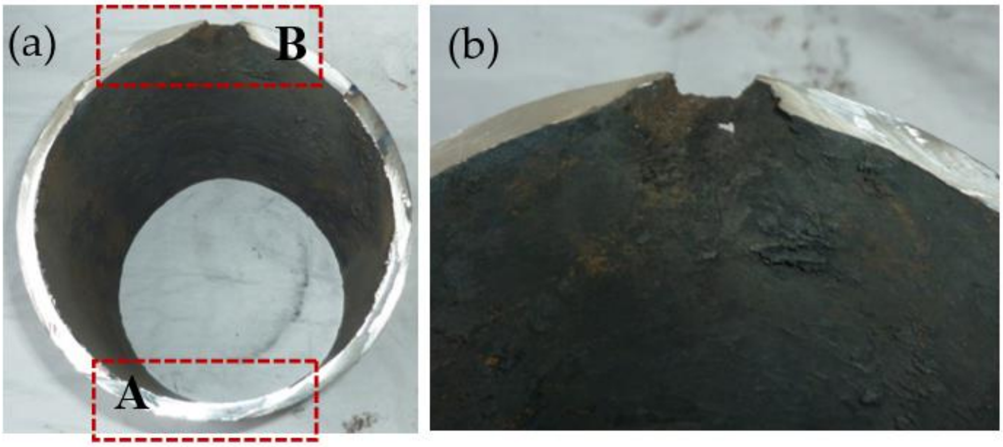

Figure 2. (a) Cross-section of the damaged tube that cutaway through one of the leakage holes, showing two areas A and B for specimen preparation, (b) Close-up view of the damaged tube around the leakage hole at area B shown in Fig. 2(a)

3. Results and Discussions

3.1. Visual and Macroscopic Examination

Close-up view of some damaged area obtained from the as-received convection tube shown in Figs. 1 and 2 showed the leakage hole(s), some remaining deposits, and a number of pits that formed at the internal tube wall. From Fig. 2, it can also be seen that the formation of the leakage hole was due to some local thinning that has occurred at the internal tube wall. In addition to a large hole shown in Fig. 1, a small hole was also observed to have formed at a location approximately close to the large hole (see also Fig. 2(b)).

3.2. Chemical Analysis

For chemical analysis, a piece of the sample was cutaway from the damaged convection tube. The result of chemical analysis obtained showed that the material used for the convection tube was met entirely to the material specification of ASTM A-106 Gr. B, see Table 1 [12].

Table 1. Result of chemical analysis obtained from the damaged convection tube material in comparison with the standard material

Element	Sample	Standard Material ASTM A-106 Gr. B
	Composition (wt. %)	
Fe	98.9	Balance
C	0.124	0.30 max
Si	0.247	0.10 min
Mn	0.438	0.29 – 1.06
P	0.0335	0.035 max
S	0.0049	0.035 max
Cr	0.0389	0.40 max
Ni	0.0478	0.40 max
Mo	0.0127	0.15 max
Nb	0.0021	-
Cu	0.0293	0.40 max
Al	0.0021	0.08 max
V	0.0129	
Ti	0.0044	-
Co	0.0293	-
W	0.0505	-

3.3. Metallographic Examination and Analysis

For metallographic examination, two areas A and B on the damaged tube were selected for specimen preparation (see Fig. 2(a)). The specimens were cut and prepared both in transverse and longitudinal sections of the tube. Area A has shown in Fig. 2(a) was located approximately at the opposite side from the leakage hole of area B.

Microstructures obtained from area A, which was located at the opposite side from the leakage hole area B, both in transverse and longitudinal sections are presented in Figs. 3 and 4, showing matrix ferrite phase (light color) with second pearlite phase (dark color), typical of low to medium carbon steels in as annealed condition [1]-[2], [11]. Most of the microstructures obtained are seen nearly equiaxed. This indicated that the tube was manufactured by hot rolling and followed by some annealing or normalizing heat treatment. Pattern and morphology of the microstructures obtained are well clearly defined and homogeneously distributed, no any metallurgical defect such as inclusion or crack observed. This clearly indicated that the tube material in area A which was located at the opposite side from the leakage hole area B was approximately still in normal condition, no any signification change or degradation in the microstructures observed. The only damage that remained seen at area A was some slight surface damage, either on the tube surface exterior or on the tube surface interior (see Figs. 3 and 4). These surface damages may have been caused by the effect of surface corrosion and or oxidation that occurred on the tube during elevated temperature service.

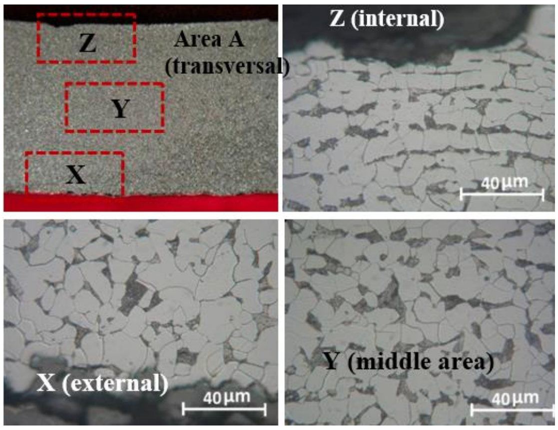

Figure 3. Microstructures at area A located approximately 180° from the leakage hole of area B (as shown in Fig. 2(a)) obtained at areas indicated by X, and Z shows all a mixture of ferrite matrix phase (light color) and second pearlite phase (dark color). Etched with 5% Nital solution

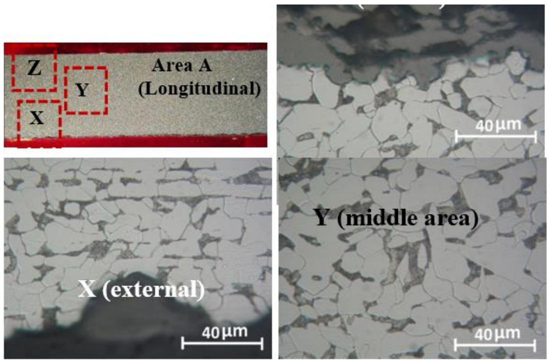

Figure 4. Macrostructure of specimen obtained from the longitudinal section at area A located approximately 180° (or at the opposite side) from the leakage hole of area B shown in Fig. 2(a). The corresponding microstructures obtained at areas indicated by X, Y and Z show all a mixture of ferrite matrix phase (light color) and second pearlite phase (dark color). Etched with 5% Nital solution

However, none of these surface damages may have significantly contributed to the thinning process that formed on the tube surface. On the contrary, the microstructures obtained from area B where the leakage hole was formed were completely different compared to the microstructures obtained from area A. The microstructures obtained in area B were no longer showing a mixture of ferrite and pearlite as in its normal condition. Still, instead most of the microstructures obtained consisted of a mix of several transformed phases such as pearlite, cementite or iron carbide and/or ledeburite together with a number of graphite nodules or graphite flakes, see Figs. 5 to 9. The formation of these microstructures was most likely caused by some carburization in which carbon was absorbed into the internal wall of the tube at an elevated temperature while in contact with a carbonaceous material or carburizing environment. The temperature that allowed diffusion of carbon into the metal was probably high enough, typically above 593 °C [5]. In carbon steels and low-alloy steels, carbon reacts to form a hard, brittle structure at the internal surface of the tube that may crack or spall upon cooling. Carburization can result in the loss of high temperature creep ductility, loss of ambient temperature mechanical properties (especially toughness/ductility), loss of weld-ability, and corrosion resistance [13].

As the microstructures change occurred only around the leakage hole area shown in Figs. 5 to 9, this indicated that the damaged convection tube had been experiencing some localized overheating or local hot spot [14]. This local hot spot may have resulted from the internal deposit build-up, causing an inadequate cooling effect of the flowing process stream. It is likely, the type of fouling deposit that built upon the internal tube wall was some carbonaceous material that promoted some carburization.

From Figs. 5 to 9, it can also be seen that the graphite formation in the microstructures had two types of morphology. First is a graphite nodule, which was observed in some middle area of the tube, and secondly is a graphite flake that was observed in some internal surface of the tube. The difference in this graphite morphology may have been influenced by the difference in sulfur content. Due to carburization, the material of steel tube which containing low sulfur content (< 0.05%) may have transformed the steel structure (iron carbide) into nodular graphite (or graphite nodules), while on the tube wall surface where sulfur content was probably high, the iron carbide was transformed into flake graphite [1]. This high sulfur content that presents in the leakage hole area of the damaged tube may have been associated with some form of scale or deposit containing higher sulfur content. The presence of this high sulfur content will be later confirmed by the results of EDS analysis obtained from the surface deposit that formed around the leakage hole area.

Furthermore, the formation of a number of graphite in the microstructures shown in Figs. 5 to 9 indicated that the damaged tube, particularly in the leakage area, had been experiencing some severe carburization as the level of carbon that may have been absorbed by the metal surface of the tube was quite high. This severe carburization was characterized by rapid metal wastage as a number of pits were found in most of the leakage hole area. Several pits that formed on the internal tube surface may have been containing sooth or graphite dust. This phenomenon is known as metal dusting, which usually occurs in the operating temperature range of 482 °C to 816 °C [10].

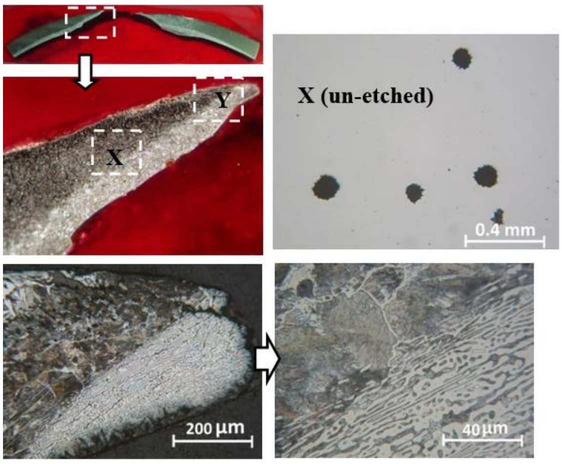

Figure 5. Microstructures obtained at the area indicated by X of un-etched specimen (as shown in Fig. 2(a)), show some formation of graphite nodules, whereas at the area indicated by Y of etched specimen shows a mixture of several transformed phases of ledeburite, iron carbide (cementite), pearlite, and some remaining ferrite and pearlite. Etched with 5% Nital solution

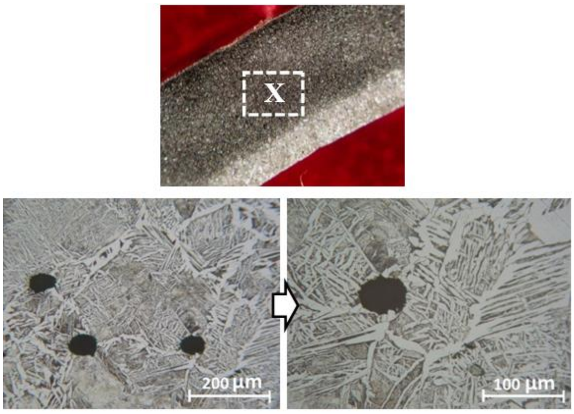

Figure 6. Microstructures of the cross-section area B (shown in Fig. 2(a)) of the leakage hole at the area indicated by X (middle area of a tube), showing a Widmanstatten structure containing several graphite nodules. Etched with 5% Nital solution

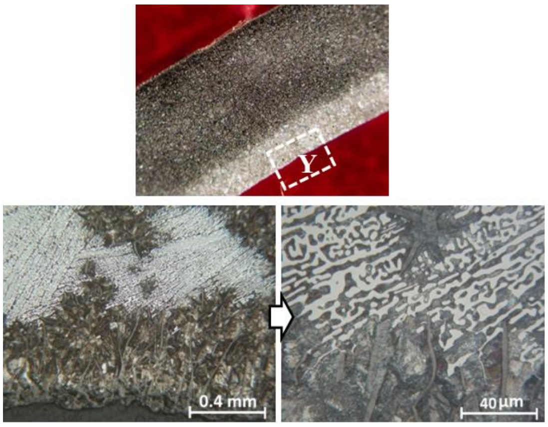

Figure 7. Microstructures of the cross-section area B (shown in Fig. 2(a)) of the leakage hole at the area indicated by Y (internal tube), showing several transformed phases of ledeburite, pearlite, iron carbide (cementite), and graphite flakes. Etched with 5% Nital solution

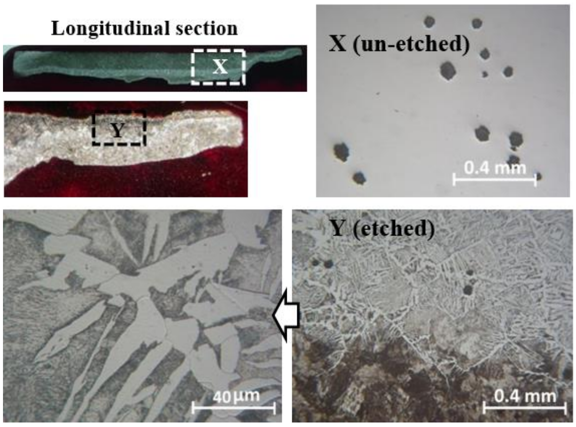

Figure 8. Macrostructure of specimen obtained from the longitudinal section of area B around the leakage hole shown in Fig. 2(a). The corresponding microstructures obtained at area indicated by X of un-etched specimen show formation of several graphite nodules (see Fig. 8(a)), whereas at area indicated by Y of etched specimen (see Fig. 8(b)) show a mixture of several transformed phases of iron carbide (cementite), pearlite, Widmanstatten structure and some graphite nodules. Etched with 5% Nital solution

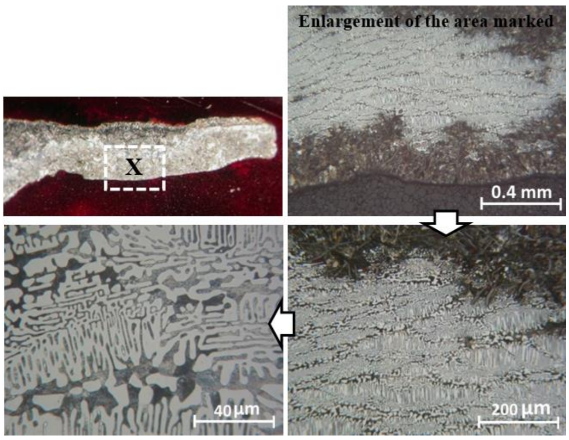

Figure 9. Microstructures obtained from the longitudinal section of specimen at area B of the leakage hole at area indicated by X, showing a mixture of several transformed phases of ledeburite, pearlite, iron carbide (cementite), and several graphite flakes at around the internal tube wall. Etched with 5% Nital solution

Table 2. Results of hardness test obtained from specimens at locations A and B at different test points of the damaged convection tube material using the Vickers hardness method (HV)

Hardness Test Location	Measured Hardness(HV) Specimen at Area A		Specimen at Area B	
	Transversal	Longitudinal	Transversal	Longitudinal
1	114.0	122.0	125.4	122.0
2	139.0	125.0	122.0	121.0
3	341.0	332.0	123.0	124.6
4	124.0	109.0		
5	127.0	148.0		
6	301.0	349.0		
7	550.0	541.0		
8	274.0	402.0		
9	441.0	165.0		
10	166.0			
11	153.0			
12	602.0			
13	642.0			
14	123.0			
15	118.0			
16	362.0			
Average	-	-	**123.5**	**122.5**

Note: Area A was located approximately 180° or at the opposite side from the leakage hole area B.

3.4. Hardness Test and Analysis

Results of hardness tests obtained from specimens of the damaged tube, either on the leakage hole (area B) or on the opposite side from the leakage hole (area A), are presented in Table 2. It can be seen that the hardness values obtained were very much different between area A and area B. The hardness values at area A were very much close to the normal condition of carbon steel tube material having ferrite and pearlite, i.e. ranging from 122.5 to 123.5 HV. On the other hand, the hardness values obtained from area B of the tube were very much different compared to those obtained from area A. Most of the hardness values obtained from area B were very much higher compared to the hardness values obtained from the normal condition of low carbon steel material. As seen in Table 2, the highest hardness value obtained in area B was up to 642.0 HV. This substantial increase in hardness value was very much associated with the formation of several transformed phases in the microstructures obtained around the leakage hole (area B), which included a mixture of pearlite, cementite, or iron carbide and/or ledeburite (see Figs. 5 to 9). These high hardness values obtained also confirmed that the area around the leakage hole was most likely subjected to some local carburization due to some localized overheating (or local hot spot) and exposure to a carburizing environment or carbonaceous material [15]. Consequently, the material around the affected area became brittle and loss in ductility and vulnerable to crack and spall upon or swept away by the flowing process stream leaving behind only the thinned or pitted metal and eventually formed the leakage hole(s). In addition, the rapid metal wastage may have also indicated by the formation of numerous graphite in the affected area as the internal tube surface had been experiencing some severe carburization or metal dusting [5] -[10].

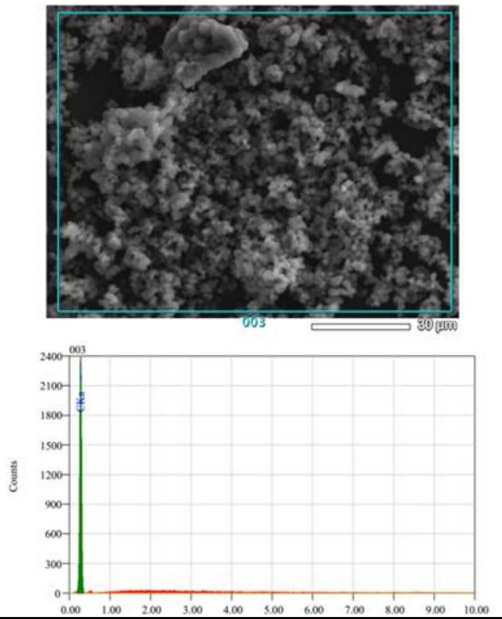

Element	Mass Percentage %
C	100.00

Figure 10. SEM and EDS analysis obtained from some deposits that formed on the damaged internal tube surface around the leakage hole area

3.5. SEM and EDS Analysis

SEM micrographs and the corresponding EDS spectrum of elements from some internal and external deposits obtained around the leakage hole area are presented in Figs. 10 and 11. From the results obtained, it is indicated that most of the deposits formed on the internal tube surface were containing major elements of carbon (C) from which the coke deposit may have formed (see Fig. 10). Coke deposits are a source of carbon that may promote carburization, particularly during decoke cycles where temperatures exceed the normal operating temperatures, accelerating the carburization [15]-[16]. On the other hand, the deposits that may have formed on the external tube surface, as seen in Fig. 11 containing with major elements of Fe, C, and O, where the other elements in small percentage may have also formed including Si, S, Ca, Al and K. Some of the elements such as S and Ca or Si may have been contributing to the oxidation, pitting and/or corrosion occurred on some external tube surface. Most of the elements containing in the external deposit may be coming from the flue gas in the heater.

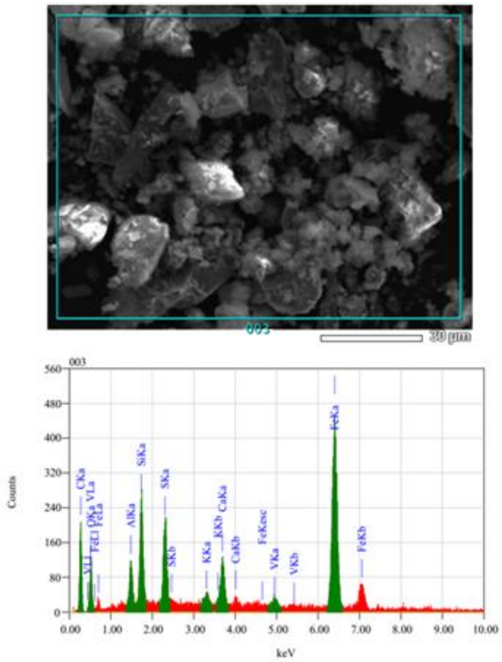

Element	Mass Percentage %
C	33.05
O	12.00
Al	2.48
Si	5.72
Ca	3.20
K	0.76
Fe	37.34
S	4.54

Figure 11. SEM and EDS analysis obtained from some deposits that formed on the damaged tube external surface around the leakage hole area

4. CONCLUSIONS

According to the damage topography and mode of failure, the convection tube had experienced some severe carburization due to the combined effect of a local hot spot or long-term localized overheating and coke deposit build-up on the internal tube surface. The local hot spot was probably affected by the formation of the coke deposit that may have caused some inadequate cooling effect of the flowing xylene to the internal tube wall, whereas the formation of the coke deposit itself was probably caused by the deposition of accumulated carbon particles from the flowing xylene in the tube. Consequently, carbon-containing in the coke deposit reacted to form a hard, brittle structure at the internal surface of the tube. The severely attacked area was later spall upon or swept away by the flowing xylene stream, leaving behind only the thinned or pitted metal and eventually formed the leakage (or through a wall) hole (s) on the tube wall. In addition, the rapid metal wastage occurred may have also indicated by the formation of numerous graphite flakes in the affected area due to some severe carburization or metal dusting.

From the results of chemical analysis obtained, it can be seen that the material used for the failed convection tube was completely met to the material specification of ASTM A-106 Gr. B. In normal condition, the microstructures of the tube material consisted of ferrite matrix phase and second pearlite phase, typical of low to medium carbon steel in as annealed condition. This was also supported by the hardness values obtained, which was in the range of 122.5 to 123.5 HV. On the other hand, the microstructures and hardness values obtained at the leakage hole area were completely different compared to the tube material in normal condition. The microstructures obtained were no longer ferrite matrix phase with second pearlite phase, but instead, the microstructures had changed completely to become a mixture of pearlite, cementite, or iron carbide and or ledeburite together with some nodule or flake graphite. It was found that hardness values of the tube material in the leakage hole area increased substantially, and the highest hardness value obtained was up to 642.0 HV.

ACKNOWLEDGEMENTS

The author wishes to express his gratitude to the Head and Members of Department of Mechanical Engineering, Faculty of Industrial Technology of the National Institute of Science and Technology (ISTN), for their support and encouragement in publishing this work.

REFERENCES

[1] Metals Handbook, "Properties and selection: Irons, steels, and high performance alloys," ASM International, Materials Park, vol.1, 10th edn., pp. 617-652, 1990.

[2] D. N. Adnyana, "Metallurgical examination and life-time assessment of high pressure steam pipes," *Metalurgi*, vol. 33, no. 3, pp. 109-124, 2018.

[3] American Petroleum Institute Standard 530, "Calculation of heater tube thickness in petroleum refineries," Washington DC, 5th edn., pp. 48-49, 2004.

[4] American Petroleum Institute RP 571, "Graphitization and softening (spheroidization)," Washington DC, 1st edn., pp. 1-7, 2003.

[5] American Petroleum Institute RP 571, "Carburization," Washington DC, 1st edn, pp. 4-113 to 4-115, 2003.

[6] H. J. Grabke, "Carburization, carbide formation, metal dusting, coking," *Materiali in Technologiye*, vol. 36, no. 6, pp. 297 - 305, 2002.

[7] C. A. Loto, R.T. Loto and A. P. I. Popoola, "An investigation of carburization resistance performance of ethylene furnace tube alloys," *Int. J. Physical Sci.*, vol. 6, no. 19, pp. 4596-4607, 2011.

[8] T. Chowwanorothapunya and C. Peeratatsuwan, "The study on high temperature degradation of AISI 1020 low carbon steel in the carburization state," *RMUTP Research Journal*, vol. 1, no. 2, pp. 22-29, 2016.

[9] G. F. Samaras and G. N. Haidemenopoulos, "Carburization of high-temperature steels: A simulation-based ranking of carburization resistance," *J. Case Stud. Eng. Fail. Anal.*, vol. 51, pp. 29-36, 2015.

[10] American Petroleum Institute RP 571, Metal Dusting, Washington DC, 1st edn., pp. 4-120, 2003.

[11] ASM Handbook, "Metallography and microstructures," ASM International, Materials Park, vol. 9, 6th print. pp. 165-216, 1995.

[12] ASME BPVC Section II Part A, "Ferrous materials specifications," The American Society of Mechanical Engineers, New York, NY, pp. 205-220, 2007.

[13] ASM Handbook, "Failure analysis and prevention," ASM International, Materials Park, vol. 11, 6th edn, pp. 1838-1849, 1998.

[14] D. N. Adnyana, "Failure of a heat exchanger return bend due to long-term localized overheating," *Metalurgi*, vol. 34, no. 1, pp. 19-30, 2019.

[15] A. P. Watkinson, "Deposition from crude oils in heat exchangers," *Proc. 6th Int. Conf. Heat Exchanger Fouling and Cleaning*, pp. 7-16, 2005.

[16] W. Wang and A.P. Watkinson, "Iron sulphide and coke fouling from sour oils: Review and initial experiments," *Proc. Int. Conf. Heat Exchanger Fouling and Cleaning*, pp. 23-30, 2011.